Trop J Nat Prod Res, October 2026; 10(10): 12555 - 12569

ISSN 2616-0684 (Print)
ISSN 2616-0692 (Electronic)



Tropical Journal of Natural Product Research

Available online at https://www.tjnpr.org

Original Research Article



Bryophyllum Pinnatum (Lam.) Oken Protects Against Oxidative Damage and Cytokine-Mediated Neuroinflammation In Pentylenetetrazole-Induced Epilepsy In Male and Female Rats

Kehinde O. Oguntunde[1,2], Adeleke K. Atunnise[1], Olusegun L. Adebayo[1]*

[1]*Department of Biochemistry, Faculty of Basic Medical Sciences, Redeemer's University, PMB 230, Ede, Osun State, Nigeria.*
[2]*Department of Biochemistry, Faculty of Science, University of Ilesa, PMB 5089, Ilesa, Osun State, Nigeria*

ARTICLE INFO

Article history:
Received 08 August 2026
Revised 19 October 2026
Accepted 22 October 2026
Published online 01 November 2026

Copyright: © 2026 Oguntunde *et al*. This is an open-access article distributed under the terms of the Creative Commons Attribution License, which permits unrestricted use, distribution, and reproduction in any medium, provided the original author and source are credited.

ABSTRACT

Epilepsy is a brain disorder characterised by unprovoked seizures arising from abnormal neuronal firing. This disorder prompts interest in medicinal plants, including *Bryophyllum pinnatum*, a Crassulaceae family, which is traditionally used for various therapeutic purposes. This study examined the neuroprotective effect of the ethyl acetate extract of *B. pinnatum* (BPE) on oxidative and inflammatory markers in brain regions, including the cortex, cerebellum and hippocampus, in pentylenetetrazole (PTZ)-induced epilepsy. Rats of both genders were randomly assigned to six groups per gender. PTZ groups were intraperitoneally injected with 40 mg/kg b.wt. PTZ on alternate days for 29 days, whereas treatment groups received 250 mg/kg BPE or 5 mg/kg b.wt. diazepam (DZP) daily. PTZ increased MDA levels by 2 - 4-fold across the brain regions, whereas BPE reduced hippocampal MDA by approximately 67% and 40% in the cortical region of PTZ-treated rats. BPE also attenuated PTZ-associated oxidative alterations, with XO activity in PTZ+BPE rats ranging from 24.2-32.2 nmol/min/mL across the investigated regions and genders, compared with 25.6-34.0 nmol/min/mL in PTZ rats. GPx activity in BPE-treated groups ranged from 5.3 to 6.3 nmol/mg protein. BPE enhanced GSH and antioxidant enzyme activities, decreased NO and pro-inflammatory markers, and elevated IL-10 and Nrf-2 levels, while preserving neuronal histoarchitecture. These findings demonstrate the neuroprotective potential of BPE against oxidative and inflammatory alterations in PTZ-induced epilepsy across both genders.

Keywords: Antioxidant, *Bryophyllum pinnatum*, Cytokine, Excitotoxicity, Neuroinflammation, Oxidative stress.

Introduction

Epilepsy is a chronic disorder in the brain, characterised by recurrent spontaneous seizures that arise from aberrant, hypersynchronous neuronal activity. [1,2] It affects over 65 million individuals globally and remains a major contributor to neurological morbidity, with higher prevalence in developing countries where diagnostic and therapeutic resources are limited. [3,4] Although seizures may occur at any stage of life, peaks are frequently observed in early childhood and late adulthood due to developmental abnormalities and cerebrovascular compromise. [5] The pathophysiological issue of epilepsy is associated with an imbalance between inhibitory and excitatory neuronal activity, primarily mediated by gamma-aminobutyric acid (GABA) and glutamate, respectively. [6,7]

Oxidative stress results in neuronal damage due to the overproduction of ROS, leading to cellular disruption and cell death through the oxidation of biomolecules. [8,9] It plays a crucial role in exacerbating injury by causing redox imbalance and thereby contributing to neuronal degeneration. It modifies glutamate receptor activity and impairs GABAergic signalling, leading to excitotoxicity within the brain. [10]

Neuroinflammation contributes to epilepsy's pathophysiology, resulting in the development of epileptic seizures. [11] This has been linked to the activation of microglia, astrocytes, and parenchymal cells, thereby releasing cytokines including Tumour Necrosis Factor-Alpha (TNF-α), interleukin-6, and interleukin-1 beta, and transcription factors such as nuclear factor-kappa B (NF-κB). These inflammatory mediators can cause brain disorders by altering neuronal excitability through disruption of glutamatergic transmission, release of excitatory neurotransmitters and alteration of the blood-brain barrier. [12,13] Furthermore, interleukin-10 (IL-10) plays a crucial modulatory role in epileptic seizures by suppressing the production of pro-inflammatory cytokines. It also inhibits inflammasome activation and reduces microglial and astroglial activation. [14]

Bryophyllum pinnatum (Lam.) Oken is locally called among major Nigerian Tribes as Abamoda in Yoruba); Ododuk mmong in Efik; Ugwoba in Igbo, and Karan in Hausa. [15] It is a succulent medicinal herb of the Crassulaceae family, which has received scientific attention for its various pharmacological activities linked to its abundant phytochemical constituents, including polyphenols, flavonoids, triterpenoids, and antioxidants such as tocopherol, quercetin, and kaempferol. [16,17] This tropical plant has demonstrated neuroprotective effects in experimental seizure models by increasing seizure threshold, reducing neuronal excitability, and attenuating oxidative and inflammatory damage. [18,19] Traditionally, *B. pinnatum* (BP) is used as an anticonvulsant and an anti-inflammatory agent. [15] Ethnopharmacological evidence indicates that this 10–15 cm elongated plant leaf powder has been used for wound healing in Nigeria. It is used locally for high blood pressure, infectious diseases such as chickenpox,

***Corresponding author. E mail: adebayool@run.edu.ng
Tel: +2348032320195

Citation: Oguntunde KO, Atunnise AK, Adebayo OL. *Bryophyllum pinnatum* (Lam.) Oken Protects Against Oxidative Damage and Cytokine-Mediated Neuroinflammation In Pentylenetetrazol-Induced Epilepsy In Male and Female Rats. Trop J Nat Prod Res. 2026;10(10): 12555 – 12569 https://doi.org/10.26538/tjnpr/v10i10.60

Official Journal of Natural Product Research Group, Faculty of Pharmacy, University of Benin, Benin City, Nigeria

© 2026 the authors. This work is licensed under the Creative Commons Attribution 4.0 International License

ISSN 2616-0684 (Print)
ISSN 2616-0692 (Electronic)

and stomach ulcers. [16,17] Also, this indigenous exotic plant has been used to treat various non-infectious conditions, particularly hypertension, diabetes, and other neurodegenerative diseases. [15]
Several antiepileptic drugs (AEDs) are known, but many of them are associated with adverse effects, including cognitive decline, neuroinflammatory responses, depression, nausea, fatigue, and dizziness with prolonged use. [20,21] Furthermore, the importance of oxidative stress as an essential mechanism for understanding epilepsy has been extensively acknowledged. [1] As a result, interest continues to grow in exploring plant-based constituents that can modulate oxidative stress and inflammatory mechanisms implicated in epilepsy with greater therapeutic potential and lower side effects. Hence, this study examined the effect of BP extract on oxidative markers and inflammatory cytokines in the cortex, cerebellum, and hippocampus of pentylenetetrazole (PTZ)-induced epilepsy in rats. This study also elucidated the sex-dependent neuroprotective mechanisms of BP and its potential therapeutic strategy in targeting oxidative and inflammatory markers in epileptic rats.

Materials and Methods

Chemicals
PTZ was purchased from Sigma-Aldrich Co., UK, and all reagents used in the experiment were of high analytical grade.

Preparation of ethyl acetate extract of Bryophyllum pinnatum
B. pinnatum (BP) was obtained from Sogunro forest, along the Deeper Life Camp area, Oyo Expressway, Ibadan, and confirmed by a botanist in the Botany Department of the University of Ibadan. A sample of *B. pinnatum* was deposited at the Departmental Herbarium unit and allotted a specimen number UIH-23263.
The ethyl acetate extract was prepared as described by Asiwe *et al.* [22] Freshly obtained leaves were dried at approximately 26 ℃ for 42 days. These were blended into a fine powder using a blender. Five hundred grams of the powder was soaked, at room temperature, in two litres of 80% methanol for 72 hours to complete the cold extraction. The crude BP extract was then filtered, distilled, and concentrated on a rotary evaporator at 40 ℃. The dried crude extract was then re-extracted with ethyl acetate and concentrated.

Phytochemicals characterisation
Fourier Transform Infrared Spectrophotometry (FTIR) analysis of B. pinnatum leaf ethyl acetate extract
The FTIR analysis was carried out on the extract using a potassium bromide pellet to crystallise it under high pressure, forming a potassium bromide (KBr) disc. The disc was placed in the FTIR spectrometer for scanning between the range of 400 - 4000 cm^{-1}.
Gas chromatography mass-spectrometry (GC-MS) analysis of Bryophyllum pinnatum ethyl acetate leaf extract
The identification of *the Bryophyllum pinnatum* ethyl acetate leaf extract was carried out using a GC-MS instrument (Shimadzu Co., Japan), GC-MS-QP2010 Ultra. The results obtained were compared using the search program of the National Institute of Standards and Technology Library (NIST). The phytochemicals with the highest similarity were identified as the compounds present. Any peak suggesting compounds with a < 50% similarity index were excluded and not presented.

Experimental procedures
Ninety-six (48 male and 48 female) albino rats weighing 150 ± 20 g were purchased from Obafemi Awolowo University's Central Animal House at Ile-Ife in Osun State, Southwest of Nigeria. The rats were acclimatised for 2 weeks and housed in stainless-steel cages. The conditions of the laboratory were maintained at 25 ± 2 ℃ and a relative humidity of 55 ± 10%, with a 12-hour photoperiod. Rats were fed *ad libitum* on the diet and given water. All procedures on animal handling followed the ethical approval for animal welfare as laid down by Redeemer's University's Animal Ethics Committee (Ethical number: RUN/REC/2024/239), which was in accordance with the ARRIVE guidelines.
Rats were assigned randomly to 6 groups, with 8 rats per group of each gender. The grouping for each gender of the rats is given below:
Control (CTR) group:Rats received normal saline.
PTZ group: Rats were injected with 40 mg/ kg b.w.t. pentylenetetrazole (PTZ) prepared in normal saline [23].
Control + BPE group:Rats were given the ethyl acetate extract of 250 mg/kg b.w.t. *Bryophyllum pinnatum* (BPE) daily.
PTZ + BPE group: Rats were treated with 40 mg/kg b.w.t. PTZ and 250 mg/kg b.w.t. BPE.
Control + DZP group: Rats were given Diazepam (DZP) daily at 5 mg/kg b.w.t.
PTZ + DZP group: Rats were treated with PTZ and DZP.
PTZ was injected intraperitoneally on alternate days for 29 days, while BPE and DZP were administered orally daily throughout the experiment. At the end of the treatments, rats were euthanised in a locally made CO_2 chamber. The brains were removed from the skulls, rinsed in cold phosphate buffer saline (PBS) (100 mM, pH 7.4), weighed, and separated into hippocampus, cerebellum, and cortex. The brain regions were kept frozen at -20 ℃ until needed for further biochemical analyses. Brain tissues from each group for histopathological analysis were removed and fixed in 10% formalin.

Sample preparations
The brain regions (hippocampus, cerebellum, and cortex) were homogenised in 10% (w/v) PBS (100 mM, pH 7.4). The homogenates were subjected to centrifugation for 15 min at 4000 rpm at 4 ℃, and the resulting supernatants were stored frozen at -20 ℃ for assessment of oxidative and inflammatory markers.

Biochemical Assays
Estimation of lipid peroxidation (LPO) level
The malondialdehyde (MDA) levels in the cortex, cerebellum, and hippocampus were measured using the procedure of Ohkawa *et al.* [24]. An equal volume of tissue homogenate from each brain region and Tris buffer (250 µL each) was mixed and incubated for two hours at a temperature of 37℃. To this mixture, 10% ice-cold trichloroacetic acid (TCA) (500 µL) was added, vortexed, and then centrifuged at 2,000 g for 10 min. Five hundred microlitres of supernatant and 500 µL of 0.67% thiobarbituric acid (TBA) were mixed and heated at 100 ℃ in a water bath for 10 min. One millilitre of distilled water was added to dilute the pink chromophore, and the absorbance was measured using a spectrophotometer at 532 nm. The results were calculated using 1.56×10^5 M^{-1} cm^{-1} as a molar extinction coefficient value and expressed as nmoles of MDA/mg protein.

Nitric oxide (NO) level estimation
The NO level was determined in the brain regions as determined by Tracey *et al.* [25] . A mixture of 50 µL of the sample, 1.5 mL of PBS (0.1 M), and 0.5 mL of Griess reagent was incubated for 15 min at room temperature. The resulting pink chromophore developed was measured at 540 nm. The results were presented as µ/mg protein.

Xanthine oxidase activity estimation
The activity of xanthine oxidase (XO) was determined using a Sigma-Aldrich kit. UK. The enzymatic colourimetric procedure was performed as described by the manufacturer's procedure.

Catalase (CAT) activity estimation
The activity of catalase (CAT) was estimated in the cortex, cerebellum, and hippocampus according to Luck. [26] The mixture, containing 3 mL of H_2O_2-phosphate buffer solution (12.5 mM hydrogen peroxide was prepared in 0.067 M sodium phosphate buffer (SPB) at pH 7.0) and 50 µL of tissue samples, was monitored by measuring the reduction in absorbance at 240 nm over 3 min. The results were calculated using a molar extinction coefficient of 71 M^{-1} cm^{-1} and presented as µmoles of H_2O_2 decomposed/min/mg protein.

© 2026 the authors. This work is licensed under the Creative Commons Attribution 4.0 International License

ISSN 2616-0684 (Print)
ISSN 2616-0692 (Electronic)

Glutathione peroxidase (GPx) activity estimation

The activity of GPx in the cortex, cerebellum, and hippocampus was estimated according to the method of Ellman [27] . The reaction (containing 200 µL of phosphate buffer (0.4 M, pH 7.0), 100 µL of sodium azide (10 mM), 200 µL of reduced glutathione (GSH 4 mM), 100 µL of H_2O_2 (0.2 mM), and 200 µL of the tissue sample) was incubated for 10 min at 37°C. After this, 400 µL of 10% (v/v) TCA was added. The reaction medium was centrifuged at 5,000 rpm for 15 min, and 1 mL of the supernatant was mixed with 0.5 mL of 0.1 mM Ellman's reagent and 3 mL of phosphate buffer (0.2 M, pH 8.0). The absorbance was measured at 412 nm, and the results were presented as nanomoles per milligram protein.

Reduced glutathione (GSH) level estimation

GSH levels were estimated in brain regions using the method of Roberts *et al.* [28] A 4% sulfosalicylic acid solution and the tissue sample mixture were centrifuged at 1,200 × g for 5 min. The supernatant (250 µL) was added to 2.25 mL of DTNB (0.1 mM) prepared in SPB, and the resulting yellow complex colour developed was read at 412 nm. GSH levels results were presented as nmol/mg protein.

Nuclear factor erythroid 2-related factor 2 (Nrf-2) quantification

Nrf-2 level in brain tissues was quantified using Nrf-2 ELISA kit (Mornmed Medical Equipment Co., Ltd, Catalogue no. MB-2877A, CHINA). Nrf-2 was quantified spectrophotometrically as described by the manufacturer's method.

Estimation of pro-inflammatory and anti-inflammatory cytokines

The interleukin-1*β* level (IL-1*β*; Elabscience, Catalogue number (CN) E-EL-R0012), interleukin-6 level (IL-6; Mornmed, CN MB-2899A), interleukin-10 level (IL-10; Elabscience, CN E-EL-R0016), tumour necrosis factor-*α* level (TNF-*α*; Elabscience, CN E-EL-R2856) and the level of nuclear factor kappa-light-chain-enhancer of activated B cells (NF-κB; Mornmed, CN MB-2878A) were measured in the cerebellum, hippocampus, and cortex of both genders. ELISA kits were used to estimate pro- and anti-inflammatory marker levels according to the manufacturer's standard procedures.

Histopathological examination

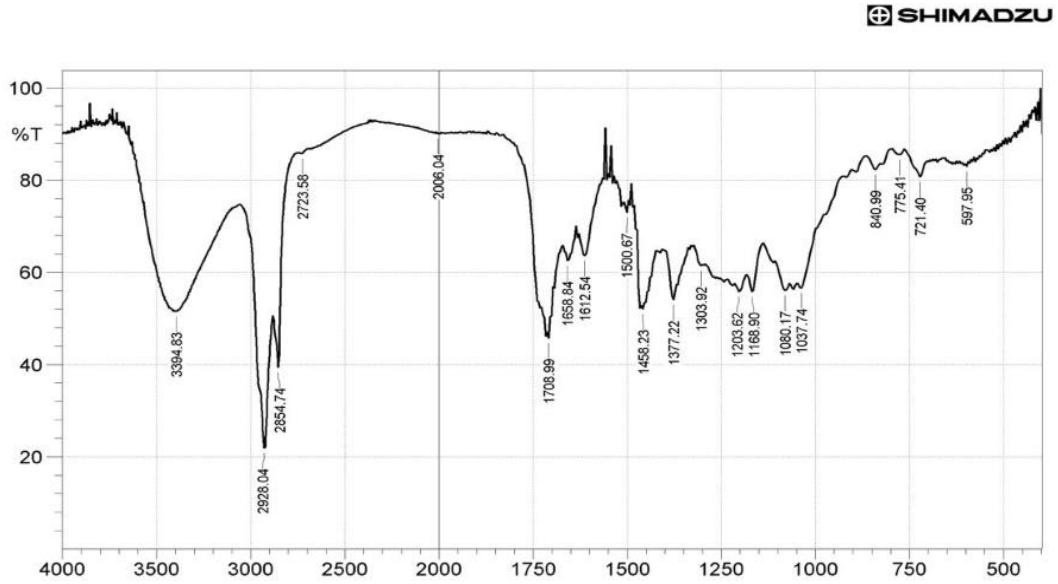
The histological examination was performed to assess changes in the cytoarchitecture of brain tissue. Whole brains from each group of animals were carefully removed, fixed in ten per cent buffered formalin, and dehydrated in graded alcohols and sectioned using a microtome at 7 µm thickness. Sections were mounted on clean glass slides and incubated at 60°C to ensure adherence. The sections were deparaffinised in xylene and then stained for 5 min with hematoxylin. Afterwards, it was washed and stained for 5 min with an eosin solution. The section was incubated for 5 min in each of the 70%, 80%, and 90% alcohol solutions. The slices were placed in 100% alcohol for 5 min, then in xylene for 1 min, and finally covered with glass slips. Microscopic examination was performed using an Olympus microscope (Tokyo, Japan) equipped with a DP71 camera. The photomicrographs of each region were taken at a X400 magnification.

Statistical analyses

Data were expressed as the mean ± SD. The results obtained from this study were analysed using one-way ANOVA in GraphPad Prism version 9 (GraphPad Software, San Diego, CA, USA). Tukey's test was adopted for post hoc multiple comparisons. This was used to assess the level of significant differences in means across groups of rats treated with PTZ, BPE, and DZP compared with their respective control rats. Values with $p < 0.05$ were considered significant.

Results and Discussion

The broad band at ~3390 cm^{-1} indicates OH functional groups of either phenolic or alcoholic. The spikes at 2928 and 2854 cm^{-1} (strong CH_2/CH_3 stretches) and bending modes around 1460 and 1377 cm^{-1} point to long or branched alkyl segments (Figure 1). A carbonyl functionality (C=O) was observed as an intense peak at 1709 cm^{-1}, and its sharpness and position are typical of esters, ketones, or carboxylic acids. Diagnostic conjugated unsaturation and aromatic features were observed at 1658 and 1621 cm^{-1}, with fingerprint patterns at 1500, 840, 754 and 721 cm^{-1}. Also, ether/ester linkages (C–O) were observed in the 1200-1000 cm^{-1} stretching region, and the broad pattern suggests multiple C–O functional groups, likely ether or ester bonds in glycosidic linkages (Figure 1).



Wavenumber (cm^{-1})	Intensity/Shape	Assignments
3394	Broad, moderate	O–H stretch of hydrogen-bonded alcohols or phenols
2928, 2854	Strong, sharp	Aliphatic C–H stretches (–CH_2– and –CH_3)
2723	Weak	Aldehyde C–H stretch
2006	Very weak shoulder	Combination/overtone bands

© 2026 the authors. This work is licensed under the Creative Commons Attribution 4.0 International License

ISSN 2616-0684 (Print)
ISSN 2616-0692 (Electronic)

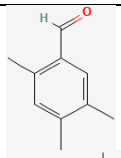
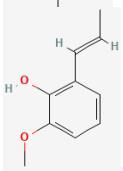
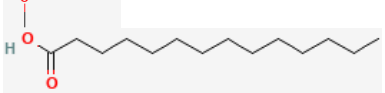
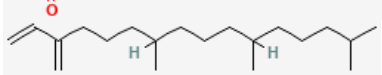
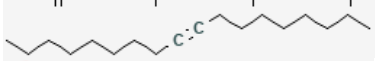
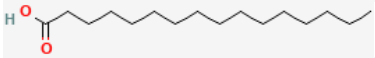
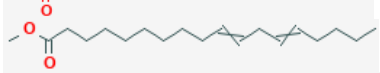
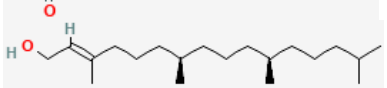
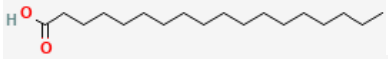
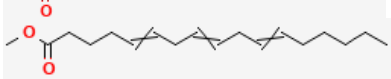
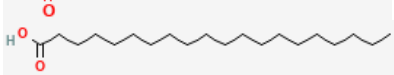
1709	Sharp, very strong	C=O stretch of ketones, esters, aldehydes, or carboxylic acids
1658, 1621	Medium, multiple peaks	C=C stretch of conjugated alkenes or aromatic ring skeleton
1500	Medium	Aromatic C=C stretching modes
1458	Medium	–CH_2– scissoring/deformation vibrations
1377	Medium	–CH_3 symmetric bending
1303	Medium	C–O stretch (ethers, phenolic –O–) or –CH_2 wag
1203, 1168	Medium	C–O stretches of alcohols, esters or carboxylic acid salts
1081, 1037	Strong	C–O–C asymmetric/symmetric stretches (ethers)
840, 754, 721	Sharp "fingerprint"	Aromatic C–H out-of-plane bends (mono- and disubstituted)
597	Weak "fingerprint"	Ring deformation or skeletal vibrations in aromatics

Figure 1: Fourier Transform Infrared Spectrum of the ethyl acetate extract of *B. pinnatum*

The data in Table 1 represent the nineteen compounds detected by GC-MS that meet the minimum detectable and quality indices, and are compared with the NIST Library. The classes of phytochemicals detected in the GC-MS analysis were: Phenol derivatives (compounds 1 and 2); fatty acids (compounds 3, 5, 6, 9, 10 and 12) and their esters (compounds 7 and 11); tocopherols (13, 14, 15 and 16); terpenoids (compounds 4 and 8) and phytosterols (compounds 17, 18 and 19).
The Structural and molecular characterisation of BPE by FTIR and GC-MS revealed complementary evidence of high polyphenol levels in the plant extract. Also, the presence of essential classes of plant secondary metabolites, including terpenoids and phytosterols, fatty acids and their derivatives, all of which are known bioactive agents, [29–31] provide structural and functional mechanistic justifications for most of the observed responses in the tissues.

PTZ treatment significantly ($p < 0.05$) elevated MDA levels in all brain regions and across both genders compared with the control group, indicating increased lipid peroxidation and oxidative stress (Figure 2), ranging from 2- to 4-fold in the female cortex to the male hippocampus, respectively. BPE treatment reduced the level of MDA significantly ($p < 0.05$) in both control and PTZ-treated rats across all brain regions and in both genders compared with the untreated groups. Among the PTZ+BPE-treated group, the hippocampus in both genders showed the largest reduction, at about 67%, while the cortex showed a 40% reduction. Similarly, DZP treatment reduced MDA levels significantly ($p < 0.05$) in the control- and PTZ-treated groups compared with their respective untreated groups.

Table 1: Gas Chromatography Mass Spectrometry (GC-MS) phytochemicals of *Bryophyllum pinnatum* ethyl acetate extract (percentage relatedness ≥ 50% and area ≥ 0.10)

S/N	Compound name	Retention time (mins)	Area (%)	Cas No.	Structures
1	Durylaldehyde	13.176	0.95	005779-72-6	
2	o-Isoeugenol	14.678	1.23	001076-55-7	
3	Tetradecanoic acid	16.595	4.03	000544-63-8	
4	Neophytadiene	16.959	5.81	000504-96-1	
5	Octadec-9-yne	17.352	2.45	035365-59-4	
6	Palmitic acid	18.334	11.73	000057-10-3	
7	10,13-Octadecadienoic acid methyl ester	19.096	1.56	056554-62-2	
8	Phytol	19.304	1.82	000150-86-7	
9	Linolenic acid	19.731	16.47	000060-33-3	
10	Stearic acid	20.061	2.48	00057-11-4	
11	methyl heptadeca-5,8,11-trienoate	20.765	1.08	022117-08-4	
12	Arachidic acid	21.233	1.91	000506-30-9	

© 2026 the authors. This work is licensed under the Creative Commons Attribution 4.0 International License

ISSN 2616-0684 (Print)
ISSN 2616-0692 (Electronic)

S/N	Compound name	Retention time (mins)	Area (%)	Cas No.	Structures
13	Alpha-Tocospiro B	24.525	2.98	601490-41-9	
14	delta-Tocopherol	25.414	4.63	000119-13-1	
15	gamma-Tocopherol	26.471	1.48	007616-22-0	
16	beta-Tocopherol, O-methyl-	27.482	3.59	1000374-73-6	
17	beta-Sitosterol	30.797	3.50	000083-46-5	
18	Simiarenol	31.605	5.03	001615-94-7	
19	delta-7,25-Stigmastadienol	32.160	1.12	006785-58-6	

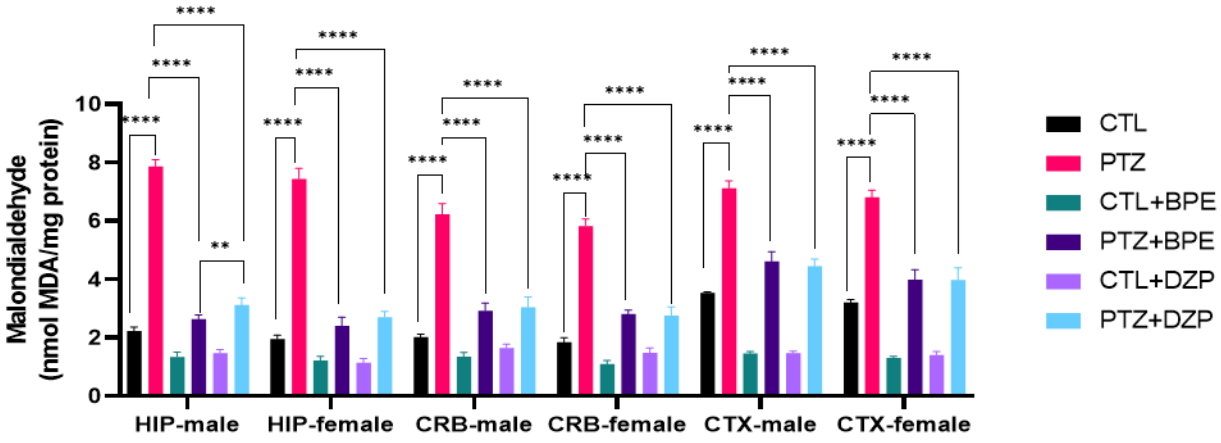


Figure 2: Effects of BPE and DZP administrations on the MDA level in the hippocampus (HIP), cerebellum (CRB), and cortex (CTX) of control and PTZ-induced seizure in male and female rats. The significant differences between the means across the groups are represented as follows: *p < 0.05, **p < 0.01, ***p < 0.001, ****p < 0.0001. Data are expressed as mean ± standard deviation and n=8.

The lipid-peroxidation-inhibitory effect of BPE may be associated with its antioxidant constituents. Experimental studies have reported that isoeugenol attenuates MDA accumulation and other oxidative-stress markers in acrylamide-induced neuropathy,[32] while phytol reduces MDA concentrations during experimental inflammation.[33] Recent evidence also supports the antioxidant activity of γ-tocopherol against lipid peroxidation,[34] and β-sitosterol has shown protective effects against diet-induced stress and lipid peroxidation in rats.[35] These findings support the possible contribution of the identified phytochemicals to the reduction in MDA observed following BPE treatment. Previous studies have reported that phenolic compounds and flavonoids in BPE contribute to its antioxidant potential by counteracting free radicals and preventing lipid peroxidation. [36,37]

The administration of PTZ significantly ($p < 0.05$) increased NO levels across all brain regions in both genders compared with controls ($p < 0.05$). The lowest elevation was 630 µmol/mg protein (in female

© 2026 the authors. This work is licensed under the Creative Commons Attribution 4.0 International License

ISSN 2616-0684 (Print)
ISSN 2616-0692 (Electronic)

cortex), and the highest was 850 µmol/mg protein in male hippocampus. Treatment with BPE and DZP attenuated NO levels significantly in PTZ-treated rats across all brain regions and genders compared to the untreated PTZ groups ($p < 0.05$) (Figure 3). Additionally, both BPE and DZP significantly ($p < 0.05$) reduced NO levels in the control and PTZ-treated rats compared with the untreated control group across all brain regions in both genders. The observed reduction in NO level suggests BPE may inhibit inducible nitric oxide synthase (iNOS), a major contributor to nitrosative stress after seizures. [38]

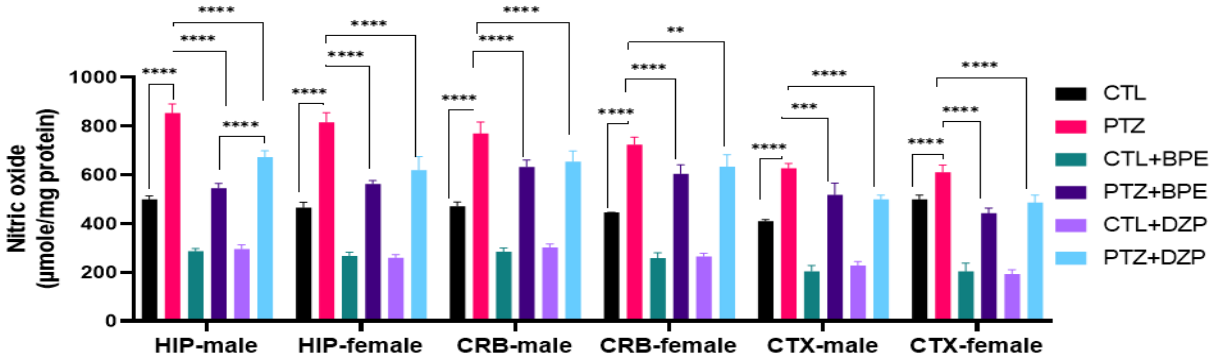


Figure 3: Effects of BPE and DZP administrations on nitric oxide (NO) level in the hippocampus (HIP), cerebellum (CRB), and cortex (CTX) of control and PTZ-induced seizure in male and female rats. The significant differences between the means across the groups are represented as follows: *p < 0.05, **p < 0.01, ***p < 0.001, ****p < 0.0001. Data are expressed as mean ± standard deviation and n=8

XO activity was significantly ($p < 0.05$) elevated in the PTZ-treated group across all brain regions. However, BPE and DZP did not affect XO activity in PTZ-treated rats. Across all the brain regions and genders, the XO activity ranged between 34.0 and 25.6 nmol/min/mL in PTZ, 32.2 and 24.2 in PTZ+BPE, and 37.5 and 26.7 in the PTZ+DZP-treated group. Also, BPE and DZP reduced XO activity in the control-treated group across all brain regions in both genders compared with the control-untreated group (Figure 4). The reason for this differential response remains unclear. The PTZ-associated increase in XO activity supports the reports by Bayrak *et al.* [39], who reported increased brain XO activity following PTZ administration in rats. Although vitamin U attenuated the PTZ-induced biochemical alterations in their study, the absence of a significant XO response to BPE and DZP in the present study indicates that these treatments did not reproduce the same effect under the experimental conditions employed.

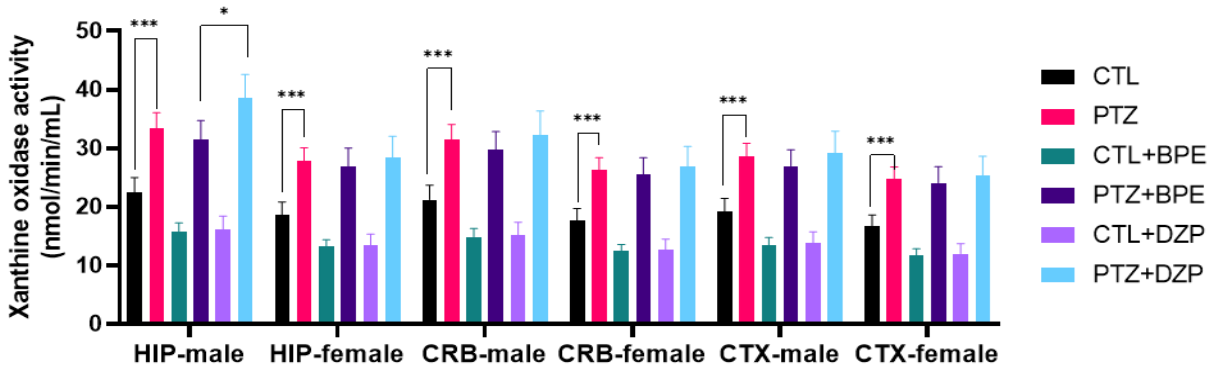


Figure 4: Effects of BPE and DZP administrations on xanthine oxidase activity in the hippocampus (HIP), cerebellum (CRB), and cortex (CTX) of control and PTZ-induced seizure in male and female rats. The significant differences between the means across the groups were indicated by *p < 0.05 and ***p < 0.001. Data are expressed as mean ± standard deviation and n=8.

Furthermore, PTZ administration reduced CAT activity significantly ($p < 0.05$) across the three regions and in both sexes. The reduced catalase activity in both genders and across the three brain regions was within the same range of 75.8 and 65.0 µmol of H_2O_2 decomposed/min/mg protein. Treatment with BPE and DZP significantly ($p < 0.05$) improved CAT activity compared to PTZ-treated rats in both genders. CAT activity in BPE- and DZP-treated groups did not differ from the control group across all brain regions in both genders ($p < 0.05$). The observed increase in CAT activity across all brain regions in the treatment groups suggests that BPE may help mitigate excess hydrogen peroxide and superoxide species, byproducts of oxidative metabolism, thereby further reinforcing the protective role of this plant across various tissues. The presence of different tocopherol isoforms in *B. pinnatum* has been reported to stimulate CAT activity, [40] which might account for the restoration observed in this study.

The activity of GPx was reduced significantly ($p < 0.05$ in the hippocampus, cerebellum, and cortex of PTZ-treated rats. Across all brain regions and in both genders, GPx activity decreased ranged between 20% - 47% in the female cortex and cerebellum, respectively. Treatment with BPE and DZP significantly ($p < 0.05$) increased GPx activity compared to PTZ rats in the hippocampus and cerebellum of both male and female groups, but the effect was not significant in the cortex of male and female rats. Also, the GPx activity in the PTZ+BPE and DZP+BPE-treated groups across both genders and brain regions was 6.3 and 5.3 nmol/mg protein in the female cerebellum and male cortex, respectively (Figure 6).

© 2026 the authors. This work is licensed under the Creative Commons Attribution 4.0 International License

ISSN 2616-0684 (Print)
ISSN 2616-0692 (Electronic)

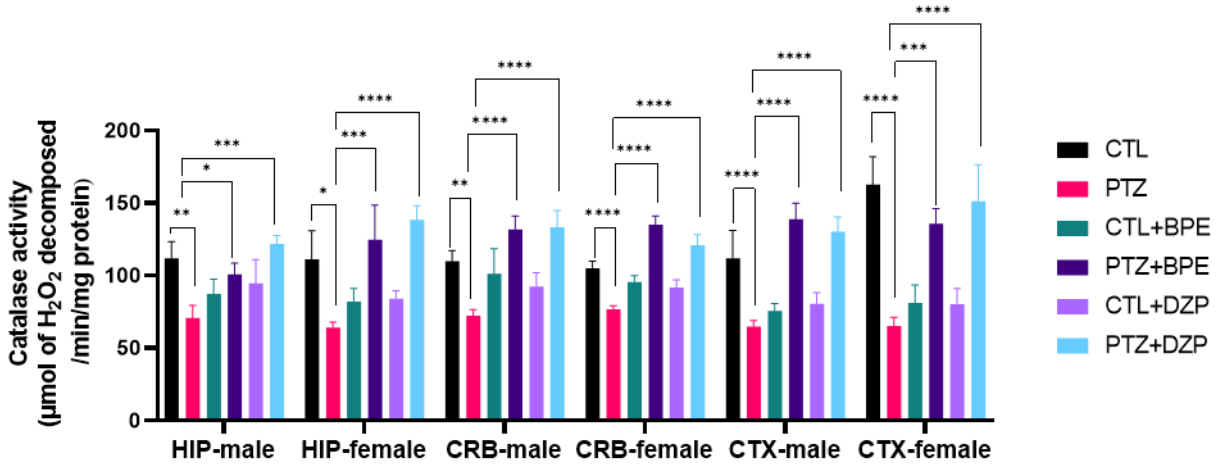


Figure 5: Effects of BPE and DZP administrations on catalase activity in the hippocampus (HIP), cerebellum (CRB), and cortex (CTX) of control and PTZ-induced seizure in male and female rats. The significant differences between the means across the groups are represented as follows: *p < 0.05, **p < 0.01, ***p < 0.001, ****p < 0.0001. Data are expressed as mean ± standard deviation and n=8

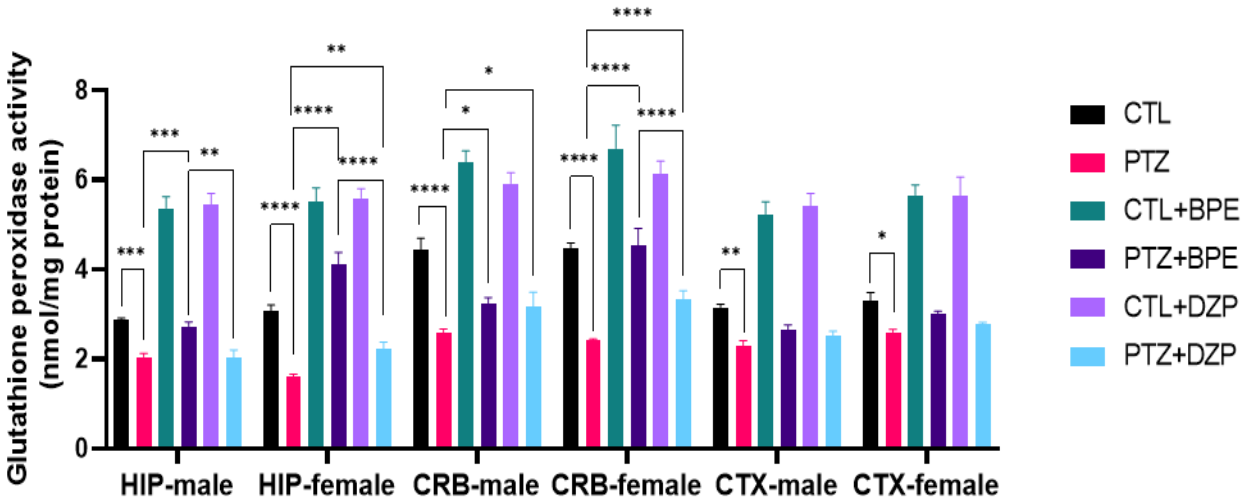


Figure 6: Effects of BPE and DZP administrations on glutathione peroxidase (GPx) activity in the hippocampus (HIP), cerebellum (CRB), and cortex (CTX) of control and PTZ-induced seizure in male and female rats. The significant differences between the means across the groups are represented as follows: *p < 0.05, **p < 0.01, ***p < 0.001, and ****p < 0.0001. Data are expressed as mean ± standard deviation and n=8

As observed in Figure 7, GSH levels in the cortex, cerebellum, and hippocampus were reduced significantly ($p < 0.05$) in the PTZ-treated group in both genders. This loss exceeded 50% across all regions of both genders. Treatment with BPE and DZP significantly increased GSH levels compared to PTZ rats. The restoration of GSH levels and GPx activity caused by oxidative injury during BPE treatment is well documented. For example, an increase in GPx activity has been reported after BPE treatment in the livers of rats induced with carbon tetrachloride, [41] which may indicate BPE's protective potential. *B. pinnatum's* protective potential may be associated with its high phenolic constituents, which have the ability to upregulate antioxidants. [42,43]

© 2026 the authors. This work is licensed under the Creative Commons Attribution 4.0 International License

ISSN 2616-0684 (Print)
ISSN 2616-0692 (Electronic)

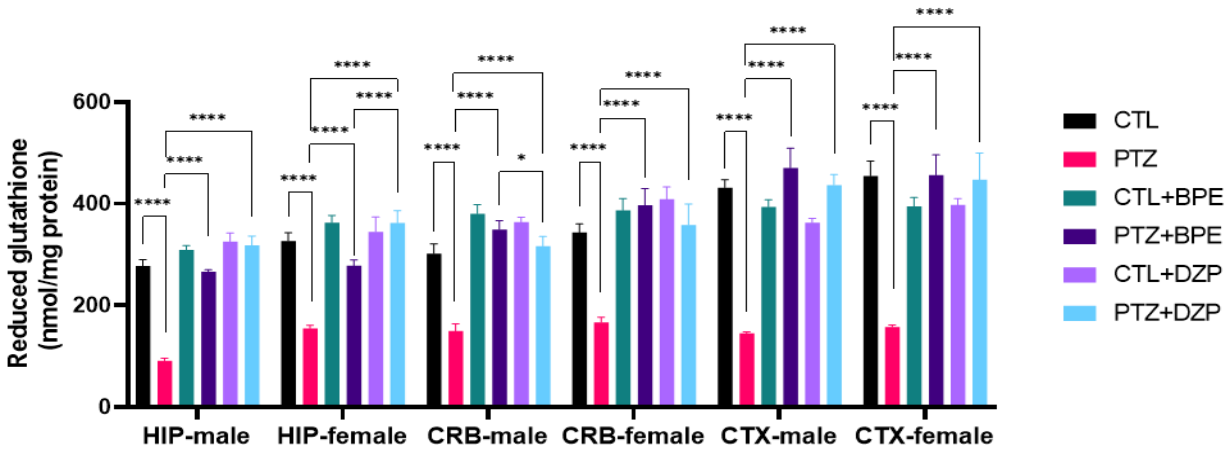


Figure 7: Effects of BPE and DZP administrations on reduced glutathione (GSH) level in the hippocampus (HIP), cerebellum (CRB), and cortex (CTX) of control and PTZ-induced seizure in male and female rats. The significant differences between the means across the groups are represented as follows: *p < 0.05, **p < 0.01, ***p < 0.001, ****p < 0.0001. Data are expressed as mean ± standard deviation and n=8.

Nrf-2 levels in the hippocampus, cerebellum, and cortex decreased significantly ($p < 0.05$) in the PTZ group than in the control group (Figure 8). The reduction was about 50% across the three brain regions of both genders. BPE and DZP treatments upregulated Nrf-2 levels in all brain regions of both genders, suggesting *B. pinnatum* as an inducer of Nrf-2. Reports have shown that Nrf-2 inducers possess protective ability against the development of neurodegenerative disease-associated brain lesions. [44,45] The BPE's neuroprotective effects may involve Nrf-2 activation, thereby restoring antioxidant defences at the transcriptional level and ultimately protecting the brain from seizure or epilepsy.

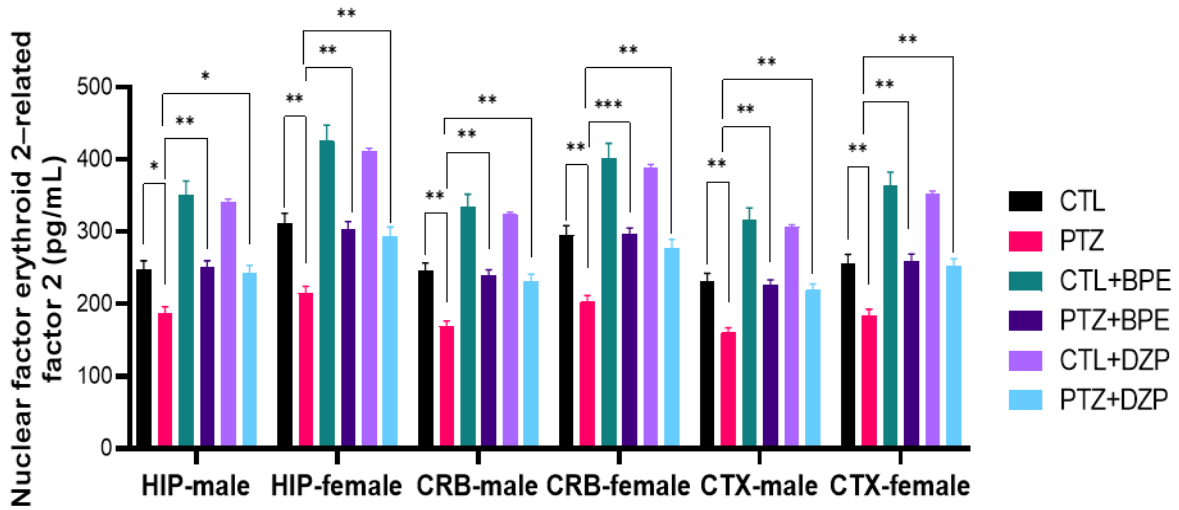


Figure 8: Effects of BPE and DZP administrations on nuclear factor erythroid 2-related factor 2 (Nrf-2) in the hippocampus (HIP), cerebellum (CRB), and cortex (CTX) of control and PTZ-induced seizure in male and female rats. The significant differences in the means across groups are indicated as follows: *p < 0.05, **p < 0.01, ***p < 0.001. Data are expressed as mean ± standard deviation, and n=8

Moreover, IL-1β level increased significantly ($p < 0.05$) in PTZ-treated rats across all brain regions when compared with the control groups (Figure 9). The IL-1β level in the male hippocampus was 94 pg/mL, the highest among the groups. The least increase in the PTZ group was observed in the female cortex (70.5 pg/mL). However, PTZ-rats treated with BPE mitigated IL-1β level across all the brain regions in both genders (except male hippocampus and female cortex) when compared to the untreated PTZ rats. Treatment with DZP, a benzodiazepine known for its anticonvulsant properties, caused a significant reduction in IL-1β levels across all brain regions in both genders compared with untreated PTZ control rats. The IL-1β counter-expression level during BPE treatment across the three regions of female and male rats in this study reflects its anti-inflammatory potential, which was comparable to that of DZP. To our knowledge, this may be the first report on the *effect of B. pinnatum* on IL-1β levels in the rat brain. Nonetheless, a neurotoxicity study by Ogidigo *et al.* [18] demonstrated that fractionated *B. pinnatum* extract protects rats against chemically induced neuronal injury, even at the transcriptional level.

© 2026 the authors. This work is licensed under the Creative Commons Attribution 4.0 International License

ISSN 2616-0684 (Print)
ISSN 2616-0692 (Electronic)

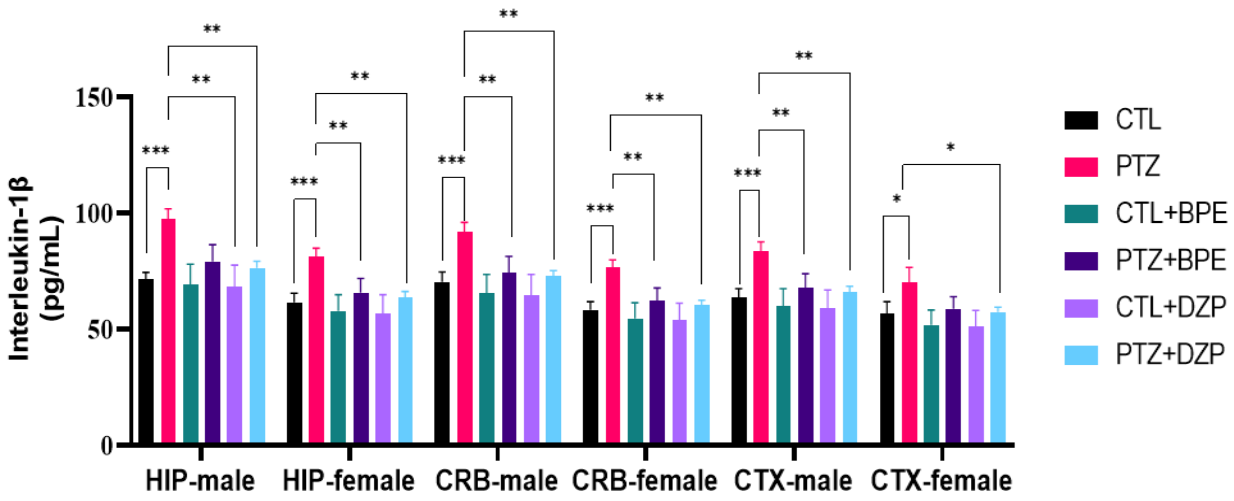


Figure 9: Effects of BPE and DZP treatments on interleukin-1β in the hippocampus (HIP), cerebellum (CRB), and cortex (CTX) of control and PTZ-induced epilepsy in male and female rats. The significant differences in the means across groups are indicated as follows: * $p < 0.05$, ** $p < 0.01$, *** $p < 0.001$. Data are expressed as mean ± standard deviation and n=8

The level of interleukin-6 (IL-6) was markedly increased ($p < 0.05$) in PTZ-treated rats across all examined brain regions in both genders compared with control rats (Figure 10). This increase ranges from 37% in the male cerebellum to 150% in the female cortex. Treatment with BPE attenuated IL-6 levels in brain regions of both genders compared with untreated PTZ rats. Furthermore, a reduction in IL-6 levels was noted in DZP-treated PTZ rats compared to untreated PTZ rats. However, treatments with BPE and DZP did not affect the control rats. The suppressive effect of IL-6 level in the cerebellum, hippocampus, and cortex in both genders suggests that BPE has anti-seizure potential by modulating upstream (IL-1β) and downstream (IL-6) cytokines, thereby reducing IL-6 expression. Several reports have shown similar anti-inflammatory effects across various rat tissues. For example, Oladejo *et al.* [46] reported that the hydro-ethanol leaf extract of BP inhibits IL-6 and IL-1β in the plasma of rats with cotton pellet-induced inflammation. Additionally, some of the GC-MS-identified constituents in this work have been directly or indirectly linked to the inhibition of these cytokines. Carvalho *et al.* [47] showed the mechanism by which phytol singly suppresses IL-6 in the spinal cord. An *in vitro* study of lipopolysaccharide-exposed microglia cell lines showed that β-Sitosterol suppresses IL-6 production. [48]

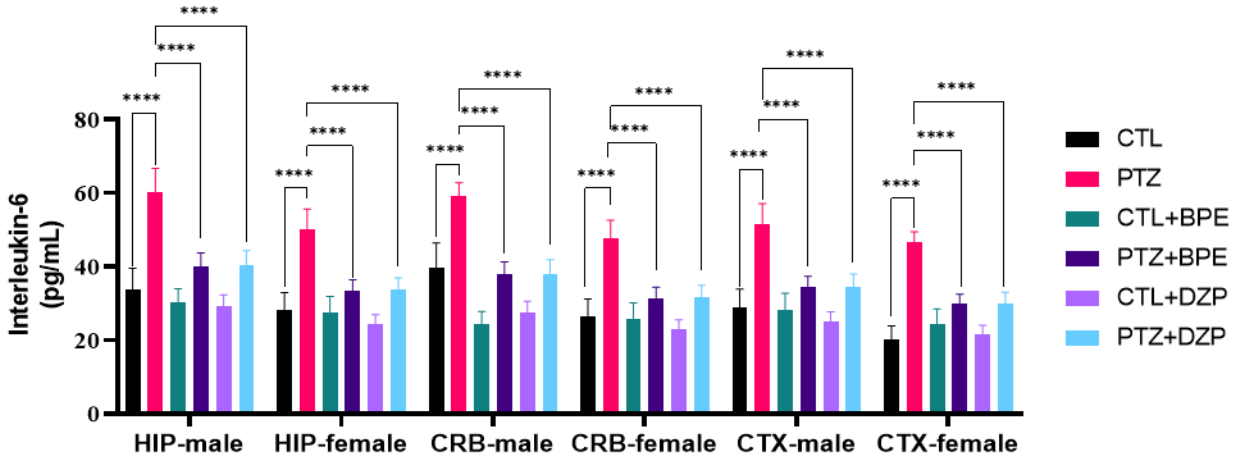


Figure 10: Effects of BPE and DZP treatments on interleukin-6 level in the hippocampus (HIP), cerebellum (CRB), and cortex (CTX) of control and PTZ-induced epilepsy in male and female rats. The significant differences between the means across the groups were represented by **** ($p < 0.0001$). Data are expressed as mean ± standard deviation and n=8

As shown in Figure 11, PTZ treatment significantly ($p < 0.05$) elevated TNF-α levels in the cortex, cerebellum, and hippocampus of both genders compared with control rats. Also, treatments with BPE and DZP significantly reduced TNF-α levels across all brain regions in male and female rats compared with the untreated PTZ group, except in the male hippocampus, where the DZP effect was not significant ($p > 0.05$). The increase in TNF-α in the brain regions of both genders was more than 50% compared with the control group. BPE and DZP treatments had no effect on the control rats compared with untreated controls. Similar to the previously discussed cytokines, the upregulation of TNF-α levels, which was reversed by BPE treatment in the selected brain regions of both genders in this study, was comparable to that observed in the DZP-treated group. A few studies have reported the anti-seizure potential of BPE in animal models, but to our knowledge, none have investigated the effect of the BP extract on TNF-α level in specific brain regions. However, there is evidence of BP's protection via TNF-α in non-epileptic animal models. [49,50]

© 2026 the authors. This work is licensed under the Creative Commons Attribution 4.0 International License

ISSN 2616-0684 (Print)
ISSN 2616-0692 (Electronic)

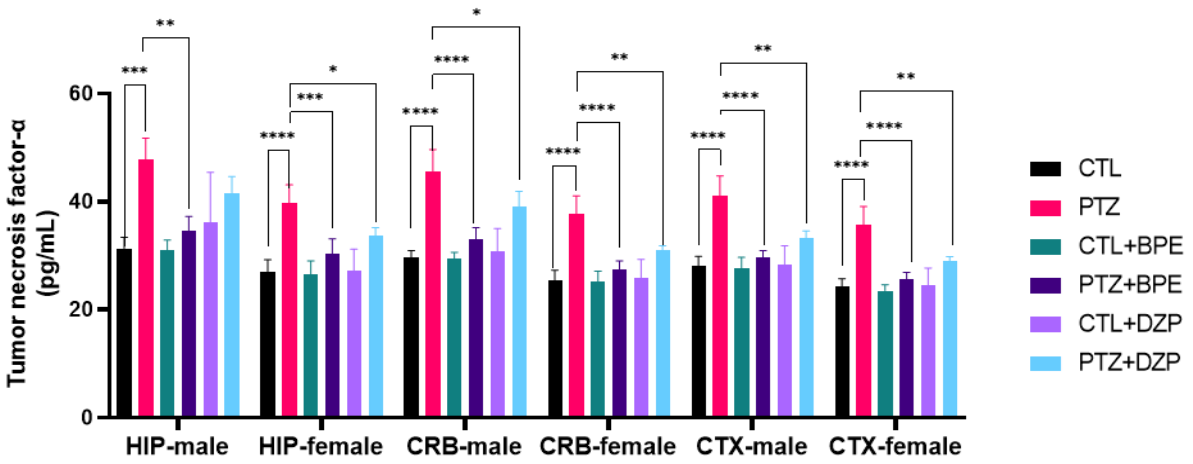


Figure 11: Effects of BPE and DZP treatments on TNF-α level in the hippocampus (HIP), cerebellum (CRB), and cortex (CTX) of control and PTZ-induced epilepsy in male and female rats. The significant differences between the means across the groups were represented as * $p < 0.05$, ** $p < 0.01$, *** $p < 0.001$, **** $p < 0.0001$. Data are expressed as mean ± standard deviation and n=8.

Furthermore, PTZ treatment significantly increases ($p < 0.05$) NF-κB levels in all brain regions compared to control rats (Figure 12). The male hippocampal NF-κB level was 538 pg/mL, and this increase remained within 30% above other regions of both genders. The treatments with BPE and DZP significantly reduced NF-κB level in PTZ-treated rats across all brain regions in both genders, indicating the efficacy of BPE and DZP in mitigating the inflammatory response associated with PTZ-induced seizures. The downregulation of IL-6, IL-1β, TNF-α, and NF-κB levels observed in this study may be due to the presence of vitamin E isoforms, α-tocopherol (αT) and γ-tocopherol (γT), in BPE. It has been reported in *in vitro* and *in vivo* experiments that both α- and γ-tocopherols possess anti-inflammatory activity, and that combining them is more potent than supplementation with αT alone. [51,52] Hence, the combined tocopherols present in the BPE may act synergistically to exert anti-inflammatory effects, as observed in this study. On the other hand, the neuronal NF-κB suppression observed in this result may be related to β-sitosterol's ability to inactivate the NF-κB pathway. [48] Zheng *et al.* [53] reported that β-Sitosterol suppresses neuropathic inflammation via the TLR4/NF-κB inhibition signalling pathway.

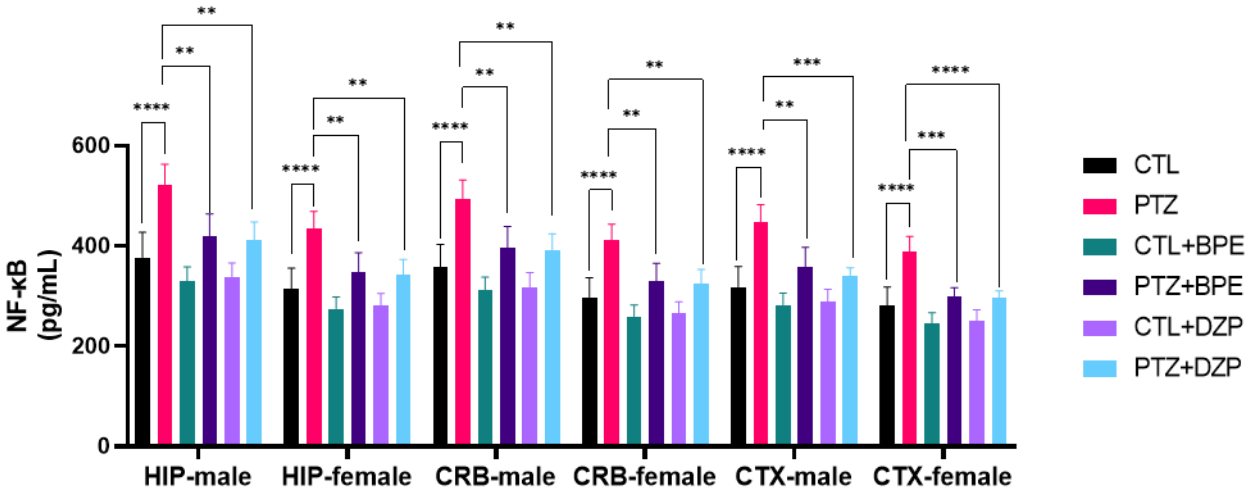


Figure 12: Effects of BPE and DZP treatments on NF-κB level in the hippocampus (HIP), cerebellum (CRB) and cortex (CTX) of control and PTZ-induced seizure in male and female rats. The significant differences between the means across the groups were represented as ** $p < 0.01$, ***$p < 0.001$, **** $p < 0.0001$. Data are expressed as mean ± standard deviation and n=8.

Figure 13 shows that PTZ treatment significantly reduced ($p < 0.05$) IL-10 levels in the hippocampus, cerebellum, and cortex of both genders compared with the control group. BPE treatment increased IL-10 levels significantly across brain regions in both genders compared with untreated PTZ control rats. The reduction in IL-10 levels across brain regions in both genders was approximately 40% lower than in the control. The treatment of the PTZ group with DZP did not significantly affect IL-10 levels, suggesting greater efficacy of BPE than DZP in restoring IL-10 levels. The upregulation of IL-10 level by BPE indicates its ability to enhance anti-inflammatory responses, which may help mitigate neuroinflammation and foster a neuroprotective milieu during epileptic seizures. This effect may be connected to the presence of bioactive compounds, particularly the isomeric form of o-isoeugenol, [54] and neophytadiene, as demonstrated in a lipopolysaccharide-induced inflammation study. [55] In addition, phytol, a component of the extract, possesses anti-inflammatory potentials, and the possible mechanism has been elucidated as involving COX-1 and 2, NF-κB, and IL-1β-dependent pathways. [56]

© 2026 the authors. This work is licensed under the Creative Commons Attribution 4.0 International License

ISSN 2616-0684 (Print)
ISSN 2616-0692 (Electronic)

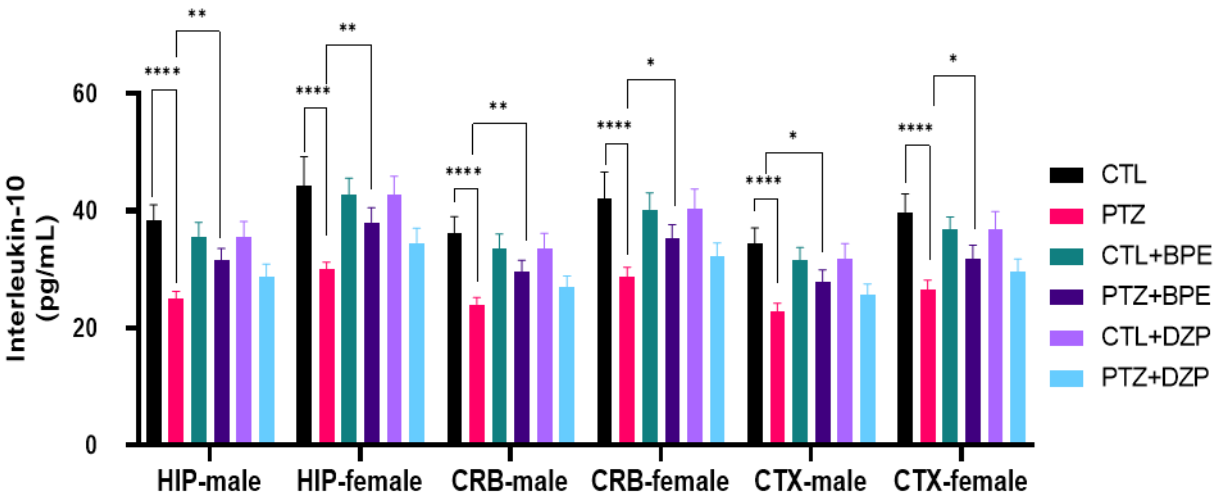


Figure 13: Effects of BPE and DZP treatments on interleukin-10 level in the hippocampus (HIP), cerebellum (CRB), and cortex (CTX) of control and PTZ-induced epilepsy in male and female rats. The significant differences between the means across the groups were represented * $p < 0.05$, ** $p < 0.01$, **** $p < 0.0001$. Data are expressed as mean ± standard deviation and n=8.

On the other hand, Figure 14a shows the representative panel of males and females' hippocampal CA3 region of PTZ-induced female and male kindling rats at x100 magnification. In the male CTL section (left panel), the CA3 pyramidal cell layer appears as a compact and continuous band of densely packed pyramidal neurons with uniform nuclear staining and preserved layer thickness. In the corresponding male PTZ section, the pyramidal layer appears less compact, with visible widening between adjacent neurons, focal irregularity in layer continuity, and the presence of more intensely stained nuclei compared to CTL. For the CTL+BPE plate, the pyramidal layer remains compact and continuous, comparable to male CTL, with closely arranged neurons and uniform staining. The male PTZ+BPE plate revealed that the pyramidal layer appears more compact and better aligned than in male PTZ, with improved continuity of the neuronal band and fewer visibly dark-stained nuclei. The male CTL+DZP group pyramidal layer is densely arranged and clearly delineated, similar to male CTL. In the male PTZ+DZP section, the pyramidal cell layer appears more continuous and compact compared to male PTZ, with reduced neuronal separation and more uniform organisation.

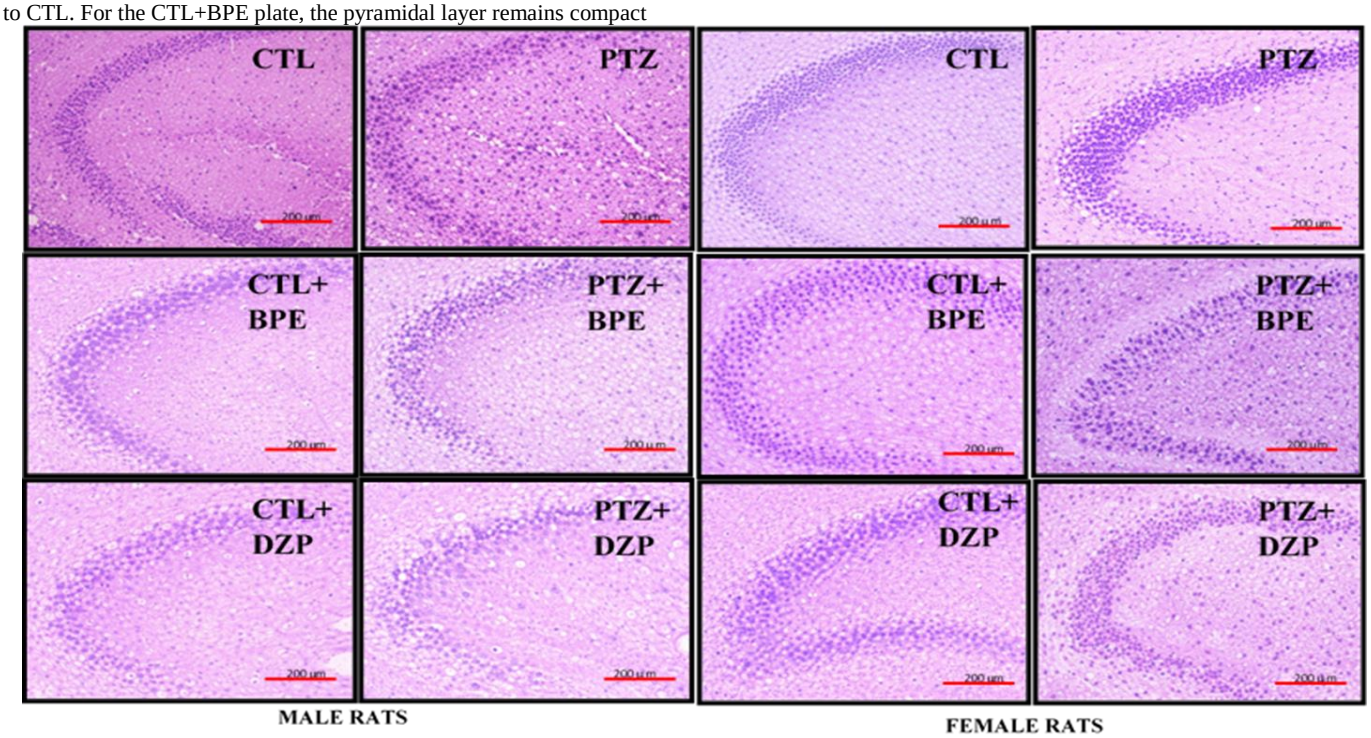


Figure 14a: Representative photomicrographs of H&E-stained sections of hippocampal CA3 region of adult male (LEFT PANEL of 6 plates) AND females (RIGHT PANEL of six plates) rats showing the effects of PTZ-induced seizures and treatment with *Bryophyllum pinnatum* extract (magnification ×100). CTL (normal saline), PTZ (pentylenetetrazole, 40 mg/kg b.w.t.), CTL+BPE and PTZ+BPE (*Bryophyllum pinnatum* extract, 250 mg/kg b.w.t., daily), and CTL+DZP and PTZ+DZP (diazepam, 5 mg/kg b.w.t.). Scale bar = 200 µm

© 2026 the authors. This work is licensed under the Creative Commons Attribution 4.0 International License

ISSN 2616-0684 (Print)
ISSN 2616-0692 (Electronic)

In the female CTL section (right panel), the CA3 pyramidal layer is compact, continuous, and uniformly stained. In the corresponding female PTZ section, the layer appears thicker and less uniformly compact, with focal dispersion of pyramidal neurons and increased prominence of darkly stained nuclei relative to female CTL. In the female CTL+BPE group, hippocampal CA3, pyramidal layer remains continuous and densely packed, comparable to that of the female CTL. The female PTZ+BPE plate showed that the pyramidal layer appears more compact and regularly arranged than in female PTZ, with improved continuity and reduced visible dispersion. In the female CTL+DZP section, the pyramidal layer is compact and orderly, similar to that of the female CTL. In the female PTZ+DZP group, the pyramidal layer appears more continuous and better organised compared to the female PTZ, with more uniform neuronal spacing and fewer visibly dark-stained nuclei.

Similarly, Figure 14b shows the representative panels of H&E-stained cerebellum of PTZ-induced female and male kindling rats at x100 magnification. The male CTL cerebellum (left panel) showed a well-preserved trilaminar organisation, consisting of a sparsely cellular molecular layer, a densely packed granule cell layer and a continuous Purkinje cell monolayer. Purkinje cells are large and flask-shaped, with distinct nuclei, while granule cells form a compact, uniformly stained band. No visible vacuolation is observed. The Purkinje cell layer appears focally disrupted with irregular spacing in the counterpart male PTZ. Within the granular layer and extending into the molecular layer, clear vacuolated spaces are visible, appearing as round to irregular pale areas interrupting the compact cellular arrangement. The granule cell layer shows reduced uniformity compared with that of the male CTL. In the male CTL+BPE group, the cerebellar layers remain distinct, with continuous Purkinje cell alignment and a compact granule cell layer similar to that of male CTL. In contrast, the male PTZ+BPE group's Purkinje cell layer appears more continuous than that in male PTZ. The granule cell layer shows fewer, smaller vacuolated spaces than in male PTZ and a more uniform cellular distribution. In the male CTL+DZP group, the trilaminar architecture is preserved, with densely packed granule cell layers and intact Purkinje cells. No obvious vacuolation is visible. Also, the male PTZ+DZP group Purkinje cell alignment appears improved relative to male PTZ, and the granule cell layer shows reduced visible vacuolated spaces compared to male PTZ.

In the female CTL cerebellum (right panel), the Purkinje cell monolayer, the molecular layer, and the granular cell layer are clearly defined and uniformly organised, with no obvious vacuolation. In the corresponding female PTZ group, vacuolated spaces are evident within the granular cell layer and focally in the molecular layer, appearing as clear, rounded areas that disrupt the dense cellular pattern. The Purkinje cell layer also showed irregular spacing compared with that of the female CTL. The female CTL+BPE group plate revealed that the trilaminar remains organised, with continuous Purkinje alignment, a compact granule cell layer, and minimal vacuolation. In the female PTZ+BPE group, fewer vacuolated spaces are visible compared to the female PTZ, and the granule cell layer appears more uniformly compact. The female CTL+DZP plate's trilaminar structure remains intact without visible vacuolation. The female PTZ+DZP plate presents some reduced vacuolated areas compared to the female PTZ, and Purkinje cell alignment appears more continuous relative to its PTZ counterpart.

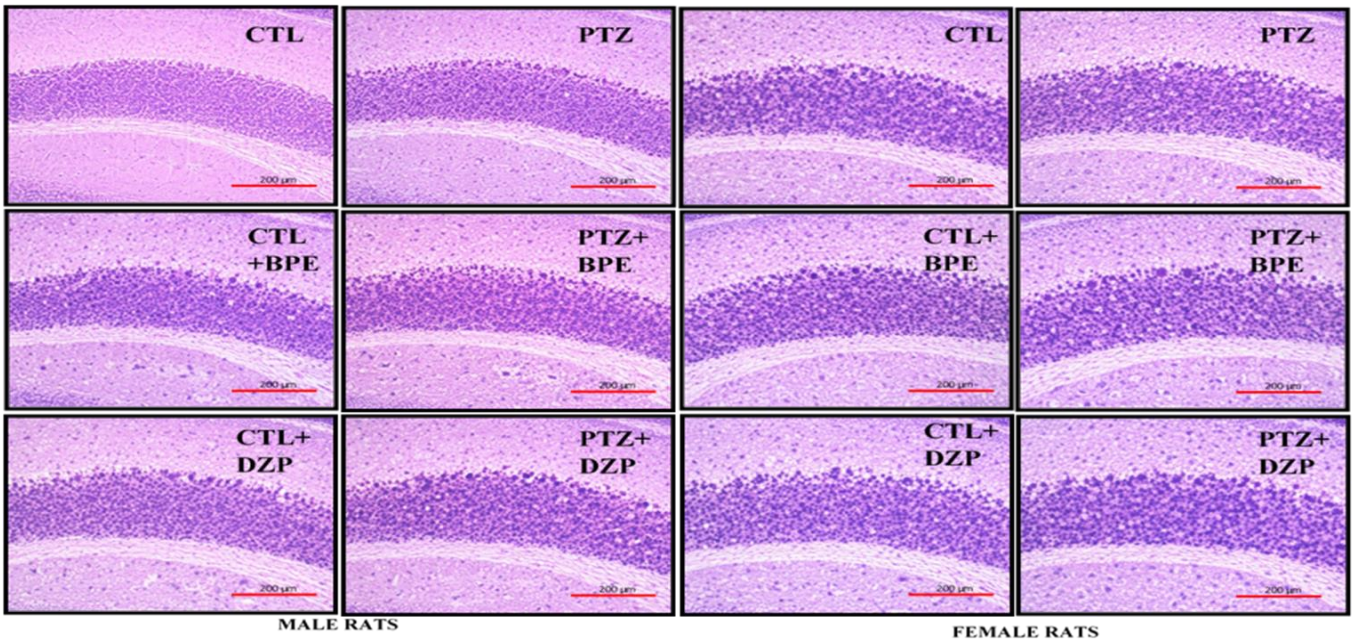


Figure 14b: Representative photomicrographs of H&E-stained sections of cerebellum of adult male and female rats showing the effects of PTZ-induced seizures and treatment with *Bryophyllum pinnatum* extract (magnification ×100). CTL (normal saline), PTZ (pentylenetetrazole, 40 mg/kg b.w.t.), CTL+BPE and PTZ+BPE (*Bryophyllum pinnatum* extract, 250 mg/kg b.w.t., daily), and CTL+DZP and PTZ+DZP (diazepam, 5 mg/kg b.w.t.). Scale bar = 200 µm

Furthermore, Figure 14c shows the representative panels of H&E-stained cortex of PTZ-induced female and male kindling rats at x100 magnification. In the male cortex (left panel), the CTL group shows a preserved cortical arrangement with evenly distributed neuronal cell bodies embedded within a relatively homogeneous neuropil. Neurons display round-to-oval somata with visible nuclei and few nucleoli. The male PTZ group shows fewer visibly intact neuronal profiles, with several neurons appearing smaller and more intensely stained (hyperchromatic). The neuropil in the PTZ section contains clear, pale spaces that disrupt its uniform appearance. The CTL+BPE group exhibits cortical architecture and neuronal morphology comparable to those of the male CTL, with preserved neuronal somata and a relatively uniform neuropil. The PTZ+BPE group, relative to the male PTZ group, shows a greater number of neurons with preserved cell body morphology and less visible hyperchromatic shrunkage, with less noticeable pale spaces within the neuropil. The CTL+DZP group appears similar to the male CTL in neuronal distribution and structural arrangement. When the PTZ+DZP group was compared with the male PTZ group, it showed fewer hyperchromatic shrunken neurons and reduced prominence of pale spaces, with less preserved cortical architecture.

© 2026 the authors. This work is licensed under the Creative Commons Attribution 4.0 International License

ISSN 2616-0684 (Print)
ISSN 2616-0692 (Electronic)

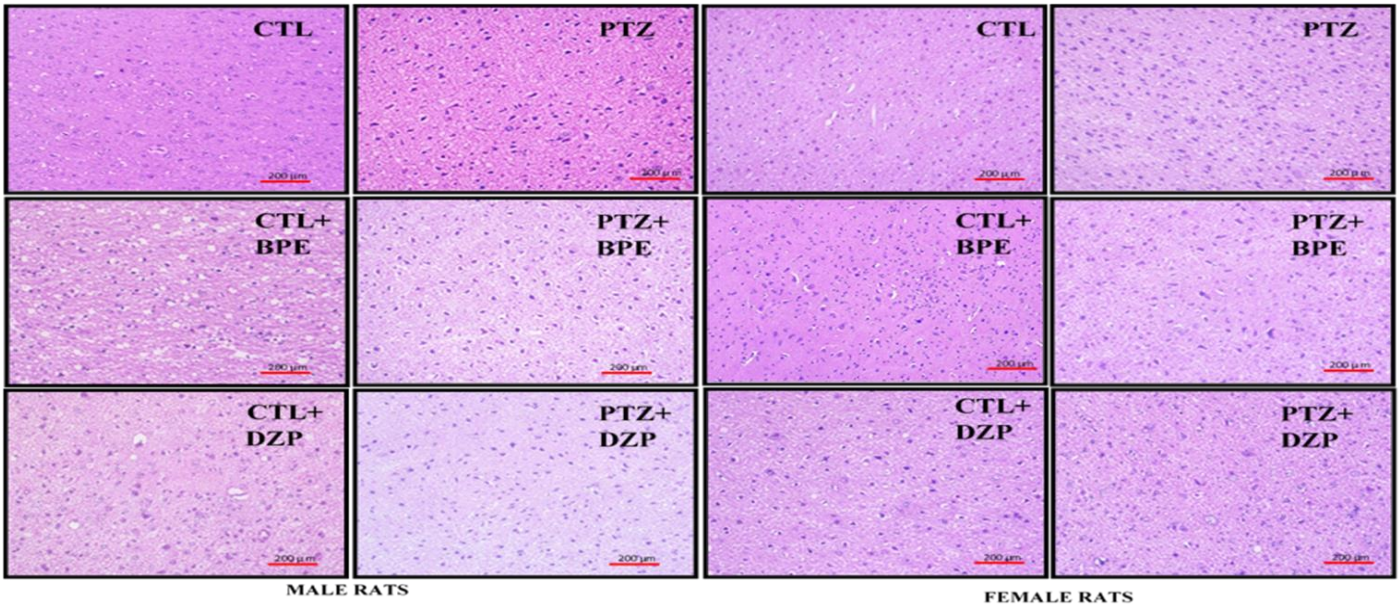


Figure 14c: Representative photomicrographs of H&E-stained sections of cortex of adult male and female rats showing the effects of PTZ-induced seizures and treatment with *Bryophyllum pinnatum* extract (magnification ×100). CTL (normal saline), PTZ (pentylenetetrazole, 40 mg/kg b.w.t.), CTL+BPE and PTZ+BPE (*Bryophyllum pinnatum* extract, 250 mg/kg b.w.t., daily), and CTL+DZP and PTZ+DZP (diazepam, 5 mg/kg b.w.t.). Scale bar = 200 µm.

In the female cortex (right panel), the CTL plate shows normal cortical cytoarchitecture with evenly dispersed neuronal cell bodies, distinct nuclei, and relatively uniform neuropil without obvious pale spaces. In contrast, the female PTZ group showed fewer visibly preserved neuronal qualities, with a significant number of neurons appearing shrunken and more intensely stained. Also, pale spaces are more noticeable within the neuropil than in the female CTL. The CTL+BPE group resembles the female CTL, as it showed a moderately preserved neuronal morphology and homogeneous neuropil. The female PTZ+BPE group showed more neurons with preserved somatic morphology, less visible hyperchromatic shrinkage, and fewer obvious pale spaces. The CTL+DZP group appears comparable to the female CTL in overall architecture and neuronal appearance. The PTZ+DZP group, compared with the female PTZ plate, showed fewer hyperchromatic, shrunken neurons, less noticeable pale spaces, and a more preserved cortical structural appearance.

The hippocampus is particularly susceptible to cytotoxic insults, which are manifested by neuronal necrosis and disruption of normal tissue architecture. [57] BPE treatment showed greater protection of nerve cells, preservation of pyramidal cell layers, and reduced astrocytosis in PTZ-induced seizure compared with the untreated PTZ group. The protective effect of BPE can be ascribed to its bioactive components. Treatment with BPE markedly improved damaged cerebellar Purkinje cells and reduced spongiosis compared with PTZ rats, indicating a neuroprotective effect. Ogundare *et al.* [58] reported that *B. pinnatum* improved cerebellar histoarchitecture of Lead acetate-induced neurotoxicity condition. Similarly, DZP-treated rats show partial restoration of normal structure and reduced gliosis, with effects comparable to those of BPE. Furthermore, treatment with BPE ameliorated cortical damage by reducing chromatolysis and neuronal necrosis, demonstrating a neuroprotective effect comparable to that of DZP. The observed improvement in Purkinje cell preservation and decreased chromatolysis may be attributed to the bioactive contents, including alkaloids, steroids, and triterpenoids, present in BPE.

Conclusion

The efficacy of *Bryophyllum pinnatum* leaf extract in both genders, compared with diazepam, highlights its potential as a natural neuroprotective alternative for addressing seizure-related oxidative damage and neuroinflammation. It may therefore serve as a multi-target anti-seizure agent, particularly for people in low- and middle-income countries. This study offers new mechanistic and pharmaceutical perspectives on *B. pinnatum* leaf extract, advancing understanding and management of seizure-induced complications.

Conflict of Interests

The authors declare no conflict of interest.

Authors' Declaration

The authors hereby declare that the work presented in this article is original and that any liability for claims relating to the content of this article will be borne by them.

Acknowledgments

The authors are grateful to Messers Tunde Oguntimehin and Gbenga Daramola for their support towards the success of this study.

References

1. Adebayo OL, Luro GE, Akeju ID, Onu CF, Fawehinmi ME, Aderemi VA, Adeleke AK. Sodium butyrate ameliorates mitochondrial oxidative stress and alterations in membrane-bound enzyme activities in pentylenetetrazole-induced kindling rat model. Metab Brain Dis. 2025;40(2):120. doi:10.1007/s11011-025-01550-9.
2. Liu X, Zhang Y, Zhao Y, Zhang Q, Han F. The Neurovascular Unit Dysfunction in the Molecular Mechanisms of Epileptogenesis and Targeted Therapy. Neurosci Bull. 2024; 40, 621–634. doi.org/10.1007/s12264-024-01193-3
3. Koirala N, Adhikari SR, Adhikari M, Yadav T, Anwar AR, Ciolac D, Shrestha B, Adhikari I, Khanal B, Muthuraman M. Assistive artificial intelligence in epilepsy and its impact on epilepsy care in low- and middle-income countries. Brain Sci. 2025;15(5):481. doi:10.3390/brainsci15050481.
4. Xu X, Sha L, Basang S, Anjiao P, Xiangyang Z, Yanxu L, Yixuan L, Lei C. Mortality in patients with epilepsy: a systematic review. J Neurol. 2025; 272, 291. doi.org/10.1007/s00415-025-13002-6

© 2026 the authors. This work is licensed under the Creative Commons Attribution 4.0 International License

5. Mastrangelo M, Bonaventura CD, Lentini G, Pisani F. An updated overview on clinical and developmental trajectories of developmental and epileptic encephalopathies: From childhood to adulthood. Seizure: Euro. J. Epsy. 2026;134:190–7. doi:10.1016/j.seizure.2025.12.009
6. Sharma G, Jangra A, Sihag S, Chaturvedi S, Yadav S, Chhokar V. *Bryophyllum pinnatum* (Lam.) Oken: unravelling therapeutic potential and navigating toxicity. Physiol Mol Biol Plants. 2024;30(9):1413-27. doi:10.1007/s12298-024-01509-7.
7. Metkus JD, Blanco T, Mohan A, Oh A, Robinson C, Bhattacharya S. Excitation-inhibition balance in diseases of the brain: role of NMDA and GABA receptors. In: A review on diverse neurological disorders. Elsevier; 2024. p. 353-83. doi:10.1016/B978-0-323-95735-9.00021-8.
8. Adebayo OL, Adenuga GA, Sandhir R. Selenium and zinc protect brain mitochondrial antioxidants and electron transport chain enzymes following postnatal protein malnutrition. Life Sci. 2016;152:145-55. doi:10.1016/j.lfs.2016.03.008.
9. Jomova K, Alomar SY, Valko R, Nepovimova E, Kuca K, Valko M. Oxidative stress and inflammation in neurodegenerative disorders. Arch Toxicol. 2026;100(10):4367–445. doi:10.1007/s00204-026-04518-5
10. El-Missiry MA, Shabana S, Ghazala SJ, Othman AI, Amer ME. Melatonin exerts a neuroprotective effect against γ-radiation-induced brain injury in the rat through the modulation of neurotransmitters, inflammatory cytokines, oxidative stress, and apoptosis. Environ Sci Pollut Res. 2021;28(24):31108-21. doi:10.1007/s11356-021-12951-5.
11. Sanz P, Rubio T, Garcia-Gimeno MA. Neuroinflammation and Epilepsy: From Pathophysiology to Therapies Based on Repurposing Drugs. Int J Mol Sci. 2024;25(8):4161. doi:10.3390/ijms25084161.
12. Shabab T, Khanabdali R, Moghadamtousi SZ, Kadir HA, Mohan G. Neuroinflammation pathways: a general review. Int J Neurosci. 2017;127(7):624–33. doi:10.1080/00207454.2016.1212854
13. Mallick R, Basak S, Chowdhury P, Bhowmik P, Das RK, Banerjee A, Paul S, Pathak S, Duttaroy AK. Targeting cytokine-mediated inflammation in brain disorders: developing new treatment strategies. Pharmaceuticals. 2025;18(1):104. doi:10.3390/ph18010104.
14. Kuo HC, Chen JS, Chao CN, Lee KF, Huang YT, Mao PC. Induction of endogenous IL-10 promotes resolution and tolerance of nitric oxide in microglia. Brain Behav Immun Health. 2025; 49:101094. doi:10.1016/j.bbih.2025.101094.
15. Sodipo OA, Usman FH, Yakubu J, Wampana B. Ethnopharmacological benefit of Nigerian indigenous *Bryophyllum pinnatum* leaf on convulsive rats. J Pharm Allied Med. 2023;1(2):98-105. doi:10.58985/jpam.2023.v01i02.13.
16. Isibor J. Phytochemistry and bioactivity studies of *Bryophyllum pinnatum*: a review. Discov chem. 2026;3(1):33. doi:10.1007/s44371-025-00360-3
17. Dhumane S, Naik T, Shelke M, Dukare K, Dhongade K. Exploring the Therapeutic Potential: Phytochemistry and Pharmacology of *Bryophyllum pinnatum*. J Drug Deliv Ther. 2024;14(2):171–7. doi:10.22270/jddt.v14i2.6282
18. Ogidigo JO, Anosike CA, Joshua PE, Ibeji CU, Nwanguma BC, Nwodo OFC. Neuroprotective effect of *Bryophyllum pinnatum* flavonoids against aluminum chloride-induced neurotoxicity in rats. Toxicol Mech Methods. 2022;32(4):243-58. doi:10.1080/15376516.2021.1995557.
19. Pattanashetti L, Donagannavar MM, Jigalur D, Patil VS. *Bryophyllum pinnatum* (L.) Pers. Modulates Multiple Neuroprotective Targets in Alzheimer's Disease: Evidence from Computational and Experimental Validation. Cell Biochem Biophys. 2025;83(4):5141–66. doi:10.1007/s12013-025-01832-0
20. Lu Y, Lin M, Ou S, Sun L, Qian K, Kuang H, Wu Y. *Astragalus polysaccharides* ameliorate epileptogenesis, cognitive impairment, and neuroinflammation in a pentylenetetrazole-induced kindling mouse model. Front Pharmacol. 2024;15:1336122. doi:10.3389/fphar.2024.1336122.
21. Rai G, Sharma S, Bhasin J, Aggarwal K, Ahuja A, Dang S. Nanotechnological advances in the treatment of epilepsy: a comprehensive review. Nanotechnology. 2024;35(15):152002. doi:10.1088/1361-6528/ad1c95
22. Asiwe ES, Igwe CU, Iheanacho KME, Onyeocha IO, Onwuliri VA. Antioxidative and free radical scavenging properties of ethyl acetate fractions of *Persea americana* seed and *Bryophyllum pinnatum* leaf. Trop J Nat Prod Res. 2021;5(8):1486-92. doi:10.26538/tjnpr/v5i8.26.
23. Rajabzadeh A, Bideskan AE, Fazel A, Sankian M, Rafatpanah H, Haghir H. The effect of PTZ-induced epileptic seizures on hippocampal expression of PSA-NCAM in offspring born to kindled rats. J Biomed Sci. 2012;19(1):56. doi:10.1186/1423-0127-19-56.
24. Ohkawa H, Ohishi N, Yagi K. Assay for lipid peroxides in animal tissues by thiobarbituric acid reaction. Anal Biochem. 1979;95(2):351-8. doi:10.1016/0003-2697(79)90738-3.
25. Tracey WR, Tse J, Carter G. Lipopolysaccharide-induced changes in plasma nitrite and nitrate concentrations in rats and mice: pharmacological evaluation of nitric oxide synthase inhibitors. J Pharmacol Exp Ther. 1995;272(3):1011-5. PMID:7534350.
26. Luck H. Catalase. In: Bergmeyer HU, editor. Methods of enzymatic analysis. New York: Academic Press; 1971. p. 885-93.
27. Ellman GL. Tissue sulfhydryl groups. Arch Biochem Biophys. 1959;82(1):70-7. doi:10.1006/0003-9861(59)90090-6.
28. Roberts JC, Francetic DJ. The importance of sample preparation and storage in glutathione analysis. Anal Biochem. 1993;211(2):183-7. doi:10.1006/abio.1993.1254.
29. Olusa AS, Oyemitan IA. Analgesic and anticonvulsant activities of the fresh young shoot essential oil of *Asparagus officinalis* L. in mice. Trop J Nat Prod Res. 2026;10(9):11421-7. doi:10.26538/tjnpr/v10i9.2.
30. Midala J, Étienne B, Ngaibi J, Kidjama N, Wangbara T, Lamare A, Njapdounke K, Sotoing Taiwe G, Ngo-Bum E. Therapeutic potential of *Daniellia oliveri* in Chronic Temporal Lobe Epilepsy with Depression: Oxidative Stress, Brain-Derived Neurotrophic Factor, Adrenocorticotropic Hormone and Monoamines. Trop J Nat Prod Res. 2026;10(9) 11631-11638. doi: 10.10.26538/tjnpr/v10i9.27.
31. Atunnise AK, Bodede O, Adewuyi A, Maharaj V, Prinsloo G, Salau BA. Metabolomics and in vitro bioactivities studies of fermented *Musa paradisiaca* pulp: a potential alpha-amylase inhibitor. Heliyon. 2024;10(3):e24659. doi:10.1016/j.heliyon.2024.e24659.
32. Prasad SN, Muralidhara. Neuroprotective efficacy of eugenol and isoeugenol in acrylamide-induced neuropathy in rats: behavioral and biochemical evidence. Neurochem Res. 2013;38(2):330-45. doi:10.1007/s11064-012-0924-9.
33. Silva RO, Sousa FBM, Damasceno SRB, Carvalho NS, Silva VG, Oliveira FRMA, Sousa DP, Aragão KS, Barbosa ALR, Freitas RM, Medeiros VR. Phytol, a diterpene alcohol, inhibits the inflammatory response by reducing cytokine production and oxidative stress. Fundam Clin Pharmacol. 2014;28(4):455-64. doi:10.1111/fcp.12049.
34. Es-Sai B, Wahnou H, Benayad S, Rabbaa S, Laaziouez Y, El Kebbaj R, Limami Y, Duval RE. γ-tocopherol: a comprehensive review of its antioxidant, anti-inflammatory, and anticancer properties. Molecules. 2025;30(3):653. doi:10.3390/molecules30030653.
35. Gumede NM, Lembede BW, Nkomozepi P, Brooksbank RL, Erlwanger KH, Chivandi E. Protective effect of β-sitosterol against high-fructose diet-induced oxidative stress and hepatorenal derangements in growing female Sprague-Dawley rats. Lab Anim Res. 2024;40(1):30. doi:10.1186/s42826-024-00215-5.
36. Okafor CE, Ijoma IK, Igboamalu CA, Ezebalu CE, Eze CF, Osita-Chikeze JC. Secondary metabolites, spectra characterization, and antioxidant correlation analysis of the polar and nonpolar extracts of *Bryophyllum pinnatum* (Lam) Oken. BioTechnologia. 2024;105(2):121–36. doi:10.5114/bta.2024.139752
37. Uahomo PO, Isirima JC. Neuroprotective Effects of *Bryophyllum pinnatum* against Ketamine-Induced Neurotoxicity in Wistar Rats:

© 2026 the authors. This work is licensed under the Creative Commons Attribution 4.0 International License

Neurochemical, Oxidative Stress, and Histological Investigation. Int Neuropsychiatr Dis J. 2024;21(6):19–40. doi:10.9734/indj/2024/v21i6452

38. Putra M, Vasanthi SS, Rao NS, Meyer C, Van Otterloo M, Thangi L, Thedens DR, Kannurpatti SS, Thippeswamy T. Inhibiting inducible nitric oxide synthase with 1400W reduces soman (GD)-induced ferroptosis in long-term epilepsy-associated neuropathology: structural and functional magnetic resonance imaging correlations with neurobehavior and brain pathology. J Pharmacol Exp Ther. 2024;388(2):724-38. doi:10.1124/jpet.123.001929.
39. Bayrak G, Turkyilmaz IB, Yanardag R. The protective effect of vitamin U on pentylenetetrazole-induced brain damage in rats. J Biochem Mol Toxicol. 2022;36(10):e23169. doi:10.1002/jbt.23169.
40. Kongkham S, Sriwong S, Tasanarong A. Protective effect of α-tocopherol on contrast-induced nephropathy in rats. Nefrologia. 2013;33(1):116-23. doi:10.3265/Nefrologia.pre2012.Nov.11736.
41. Alli Smith YR, Aluko BT, Owolabi OV. Evaluation of antioxidant activities of aqueous extract from *Bryophyllum pinnatum* on carbon tetrachloride-induced albino rat tissues. J Drug Deliv Ther. 2021;11(4):10-5. doi:10.22270/jddt.v11i4.4877.
42. Faloye TO, Oladunmoye MK, Omoya FO. Evaluation of antibacterial and phytochemical properties of *Bryophyllum pinnatum* (Lam.) on bacteria associated with urinary tract infections. J Med Sci Biol Chem. 2025;2(1):38-47. doi:10.69739/jmsbc.v2i1.398.
43. Mukherjee S, Banik SK, Chakraborty S, Das T, Choudhury MD, Tripathi A. *Bryophyllum pinnatum* induces p53-dependent apoptosis of colorectal cancer cells via increased intracellular ROS and G2/M cell-cycle arrest in vitro and validated in silico by molecular docking. Cell Biol Int. 2025;49(5):534-54. doi:10.1002/cbin.70004.
44. Manavi MA, Jafari RM, Shafaroodi H, Dehpour AR. The Keap1/Nrf2/ARE/HO-1 axis in epilepsy: crosstalk between oxidative stress and neuroinflammation. Int Immunopharmacol. 2025;153:114304. doi:10.1016/j.intimp.2025.114304.
45. Sandouka S, Shekh-Ahmad T. Induction of the Nrf2 pathway by sulforaphane is neuroprotective in a rat temporal lobe epilepsy model. Antioxidants. 2021;10(11):1702. doi:10.3390/antiox10111702.
46. Oladejo AA, Ikechuckwu OE, Aritetsoma OH, Samuel OC, Uche OC. Inhibitory effects of *Bryophyllum pinnatum* leaf extract on inflammatory biomarkers. J Adv Med Pharm Sci. 2021;23(2):7-13. doi:10.9734/jamps/2021/v23i230218.
47. Carvalho AMS, Heimfarth L, Pereira EWM, Oliveira FS, Menezes IRA, Coutinho HDM, Picot L, Antoniolli AR, Quintans JSS, Quintans-Junior LJ. Phytol, a chlorophyll component, produces antihyperalgesic, anti-inflammatory, and antiarthritic effects: weighted MR imaging. J Cereb Blood Flow Metab. 2015;35(11):1836-45. doi:10.1038/jcbfm.2015.137.
58. Ogundare S, Bamgbose O, Ogundare EI, Ehiremen SE, Asibor E, Idehen C, Echekwube M, Obohwemu K, Airhomwanbor K, Augustine E, Iyevhobu K. A Study of Some Ameliorative Effects of Aqueous Extract of *Bryophyllum pinnatum* in Lead Acetate Induced Neurotoxicity in the Cerebellum of Adult Wistar Rats (Rattus norvegicus). Int J Med Sci Health Res. 2025; 09: 58-73. doi:10.51505/ijmshr.2025.9205

possible NF-κB pathway involvement and reduced levels of the proinflammatory cytokines TNF-α and IL-6. J Nat Prod. 2020;83(4):1107-17. doi:10.1021/acs.jnatprod.9b01116.
48. Sun Y, Gao L, Hou W, Wu J. β-sitosterol alleviates inflammatory response via inhibiting the activation of ERK/p38 and NF-κB pathways in LPS-exposed BV2 cells. BioMed Res Int. 2020;2020:7532306. doi:10.1155/2020/7532306.
49. Nurdiana DTWI, Syaban MFR, Mustafa SA, Ikhsani H, Syafitri FE, Hapsari NK, Khoirunnisa A. Efficacy and side effects studies of *Bryophyllum pinnatum* leaves ethanol extract in pristane-induced SLE BALB/c mice model. AIP Conf Proc. 2019;2108(1):020016. doi:10.1063/1.5109991.
50. Ijatuyi TT, Lawal AO, Akinjiyan MO, Ojo FM, Koledoye OF, Agboola OO, Dahunsi DT, Folorunso IM, Elekofehinti OO. Effects of *Bryophyllum pinnatum* on dysfunctional autophagy in rat lungs exposed to zinc oxide nanoparticles. Int Immunopharmacol. 2024;141:113005. doi:10.1016/j.intimp.2024.113005.
51. Mathur P, Ding Z, Saldeen T, Mehta JL. Tocopherols in the prevention and treatment of atherosclerosis and related cardiovascular disease. Clin Cardiol. 2015;38(9):570-6. doi:10.1002/clc.22422.
52. Reiter E, Jiang Q, Christen S. Anti-inflammatory properties of α- and γ-tocopherol. Mol Aspects Med. 2007;28(5-6):668-91. doi:10.1016/j.mam.2007.01.003.
53. Zheng Y, Zhao J, Chang S, Zhuang Z, Waimei S, Li X, Chen Z, Jing B, Zhang D, Zhao G. β-sitosterol alleviates neuropathic pain by affect microglia polarization through inhibiting TLR4/NF-κB signaling pathway. J Neuroimmune Pharmacol. 2023;18(4):690-703. doi:10.1007/s11481-023-10091-w.
54. Mateen S, Shahzad S, Ahmad S, Naeem SS, Khalid S, Akhtar K, Rizvi W, Moin S. Cinnamaldehyde and eugenol attenuates collagen-induced arthritis via reduction of free radicals and pro-inflammatory cytokines. Phytomedicine. 2019;53:70-8. doi:10.1016/j.phymed.2018.09.004.
55. Bhardwaj M, Sali VK, Mani S, Vasanthi HR. Neophytadiene from *Turbinaria ornata* suppresses LPS-induced inflammatory response in RAW 264.7 macrophages and Sprague-Dawley rats. Inflammation. 2020;43(3):937-50. doi:10.1007/s10753-020-01179-z.
56. Islam MT, Ayatollahi SA, Zihad SMNK, Sifat N, Khan MR, Paul A, Salehi B, Islam T, Mubarak MS, Martins N, Sharifi-Rad J. Phytol anti-inflammatory activity: preclinical assessment and possible mechanism of action elucidation. Cell Mol Biol. (Noisy-le-grand). 2020;66(4):264-9. PMID:32583784.
57. Bartsch T, Döhring J, Reuter S, Finke C, Rohr A, Brauer H, Deuschl G, Jansen O. Selective neuronal vulnerability of human hippocampal CA1 neurons: lesion evolution, temporal course, and pattern of hippocampal damage in diffusion-

© 2026 the authors. This work is licensed under the Creative Commons Attribution 4.0 International License